Deformation and Ductile Fracture of a Low Alloy Steel under High Strain Rate Loading

L. W. Meyer[1], S. Abdel-Malek[2]

[1] Chair Materials and Impact Engineering, Chemnitz University of Technology, Germany
[2] Nordmetall GmbH Research and Consulting, Burkhardtsdorf, Germany,
www.nordmetall.net

Abstract

Ductile failure of metals always occurs after a specific amount of plastic deformation. Therefore, the investigation and characterization of the deformation behaviour is required to understand the damage process and to describe the failure by a suitable constitutive relation. The effects of temperature and strain rate on the mechanical properties are important for the description of the material behavior in many applications. The MTS model is used here to describe the material behavior of some low alloy steels in a wide range of temperature and strain rates. A new part of stress is added to the MTS model in order to consider the effect of the dynamic strain aging at low strain rate and high temperature.

The determination of material data at high strain and high strain rate is needed to describe the real material behaviour, specially for the simulation of high deformation and fracture. A special technique is used here to stop the deformation of tension specimen at high strain rate in the necking zone to determine the true stress and true strain.

Using FEM computations (LS-DYNA 3D), the stress triaxiality in the necking zone of a tensile specimen is calculated up to the crack initiation. It is shown that the strain hardening characteristics affect the development of stress triaxiality.

Keywords:

High strain rate, High plastic deformation, Ductile failure

1 Introduction

Mechanical testing gives information about material behaviour at different temperatures and strain rates. The results are needed for the numerical analysis and the simulation of high strain rate deformation processes such as automobile crash tests or high speed metal forming processes. For these processes the range of relatively high strains and very

high strain rates is of great interest. In the high strain rate range, the flow stresses are influenced by the temperature increase during the deformation process. The major part of the deformation energy is transformed into heat, leading to a reduction of the flow stress. A precise description of the material behavior does not only need a good agreement of the constitutive model with the experimental results at high strain rates, but also at high deformations. Dynamic strain aging will be active in a limited range of strain rate and temperature and leads to an enhancement of the flow stresses. This must be considered in the material model.

At ductile fractures the material can fail due to the coalescence of voids, which occurs through three mechanisms: 1) squeezing of the matrix between voids, 2) nucleation and growth of secondary voids, and 3) shearing between voids. Factors affecting the ductile failure are: stress state, temperature, strain rate, twin formation, and dynamic strain aging. Understanding these effects allows forecasting how and when failure occurs. This leads to a successful modeling of failure in a numerical simulation.

2 Material model

Accurate modeling of deformation processes of materials over a wide range of strain rates and temperatures requires a reliable constitutive description of the stress-strain behavior. Several physically and empirically based models have been developed for use in computational codes [1]. Most models are use a constant strain hardening exponent n, which leads to higher flow stresses with increasing deformation. The MTS model “Mechanical Threshold Stress”, which was developed by Follansbee et al. [2], is a physically based model. It is considering that the flow stress at a certain temperature and strain rate do not increase above a saturation stress. In the MTS model the flow stress is a sum of three parts: an athermal stress σ_a, a thermal stress σ_i for the interaction of dislocations with interstitial obstacles, and a threshold stress $\hat{\sigma}_\varepsilon$ for the dislocation/dislocation interaction:

$$\frac{\sigma}{\mu} = \frac{\sigma_a}{\mu_0} + S_i\left(\dot{\varepsilon},T\right)\cdot\frac{\sigma_i}{\mu_0} + S_\varepsilon\left(\dot{\varepsilon},T\right)\cdot\frac{\hat{\sigma}_\varepsilon}{\mu_0} \tag{1}$$

μ is the temperature-dependent shear modulus and μ_0 is the shear modulus at 0 K. S_i and S_ε are factors expressing the effect of temperature and strain rate in a general form as:

$$S_{i,\varepsilon} = \left\{1 - \left[\frac{kT}{g_{0i,\varepsilon}\mu b^3} ln\left(\frac{\dot{\varepsilon}_{0i,\varepsilon}}{\dot{\varepsilon}}\right)\right]^{1/q_{i,\varepsilon}}\right\}^{1/p_{i,\varepsilon}} \tag{2}$$

While σ_a and σ_i are taken as constants, the threshold stress $\hat{\sigma}_\varepsilon$ is a state parameter and treated differentially according to:

$$\theta = \frac{d\hat{\sigma}_\varepsilon}{d\varepsilon} = \theta_0(\dot{\varepsilon})\left(1 - \frac{tanh\left(\alpha \frac{\hat{\sigma}_\varepsilon}{\hat{\sigma}_{\varepsilon s}(\dot{\varepsilon},T)}\right)}{tanh(\alpha)}\right) \tag{3}$$

where θ is the strain hardening and $\hat{\sigma}_{\varepsilon s}$ is the saturation stress. A detailed discussion of MTS model and how to determine the parameter is explained by Follansbee et al. [2-4].
At high temperatures or low strain rates the dynamic strain aging affects the flow stress. In order to consider this effect, we suggest a forth stress part to be added to the MTS model. The equation (1) shall be written as:

$$\frac{\sigma}{\mu} = \frac{\sigma_a}{\mu_0} + S_i(\dot{\varepsilon},T)\cdot\frac{\sigma_i}{\mu_0} + S_\varepsilon(\dot{\varepsilon},T)\cdot\frac{\hat{\sigma}_\varepsilon}{\mu_0} + \frac{\sigma_{DSA}}{\mu} \tag{4}$$

where σ_{DSA} is a stress part, which results from the Dynamic Strain Aging. It will be expressed with the following equation so that it is only active in the region of the dynamic strain aging, fig. 1.

$$\frac{\sigma_{DSA}}{\mu} = \frac{\sigma_{D0}}{\mu_0}\cdot sec\,h[K_1\cdot S_i(\dot{\varepsilon},T) - K_2] \tag{5}$$

σ_{D0}, K_1, and K_2 are constants, which will be determined by using the difference of experimental data σ_{exp} and the σ_{MTS} data calculated with equation (1).

$$\sigma_{DSA} = \sigma_{exp} - \sigma_{MTS} \tag{6}$$

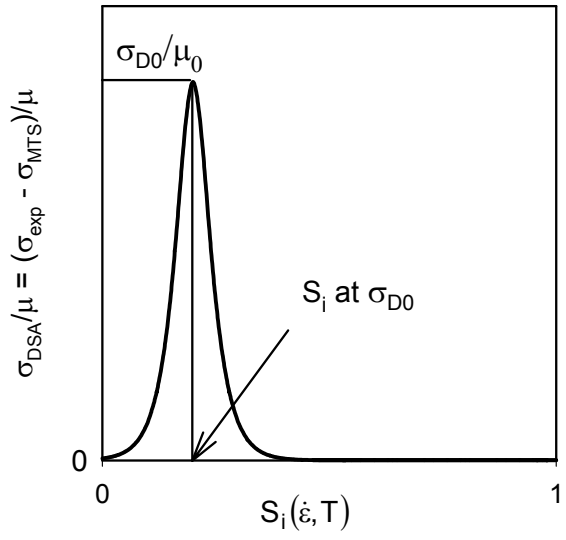

***Figure 1**: Relationship between σ_{DSA} and $S_i(\dot{\varepsilon},T)$*

3 Experimental procedures

Tension tests were carried out on four high strength low alloyed steels under quasistatic and high rate loading conditions. Tensile tests at low and medium velocities were done with the proved 250 kN hydraulic test machine Instron 8503, which has a large test velocity range of v = 0.005 up to 800 mm/s.

Dynamic tensile tests were performed on the rotating wheel machine at different velocities. The rotating wheel machine consists of a flywheel (200 kg) with a claw, which is released at the required test velocity and is impacting a yoke. The yoke pulls the test specimen, which is attached in a specimen holder. The force measurement is applied directly beside the gage length with strain gages. The strain was measured directly with strain gages. Because of the high energy capacity of this apparatus the test velocity is constant up to failure even for high strength, high ductility materials. For more details see Meyer et al. [5].

Only flow stresses up to UTS are used to get the parameter of the MTS model. To verify the material model at high deformations, the high rate tensile test was interrupted in the necking region using a special stopping device. The stress is calculated from the measured force and the actual area of the smallest cross section and corrected to the uniaxial stress state according to Bridgman [6].

A characterization of the ductile failure behavior was performed by using notched specimens, which were tested under tensile loading with three speeds; v = 0.1 mm/s, 5 m/s, and 25 m/s. The changes in the minimum diameter at the notch root were used as a criterion to measure the effective strain at failure.

4 Results and discussion

4.1 Modeling the flow stress

The parameters of the MTS model, eq. (1), were determined by using the results of the tension tests up to UTS in the strain rate range 10^{-4} s^{-1} to $5 \cdot 10^{3}$ s^{-1}. For high strain values interrupted dynamic tensile tests were carried out with a test speed of 5 m/s. The required strain value is adjusted with a special device, which guides the deformation process into a secondary specimen, the so-called sacrifice specimen, which fails and leaves the test specimen only deformed with a necking. The flow stress and strain are calculated with the actual force and cross sectional area and corrected to the uniaxial stress state according to Bridgman [6]. An advantage of this method is the consideration of the adiabatic status resulting from the heating of the specimen under dynamic conditions.

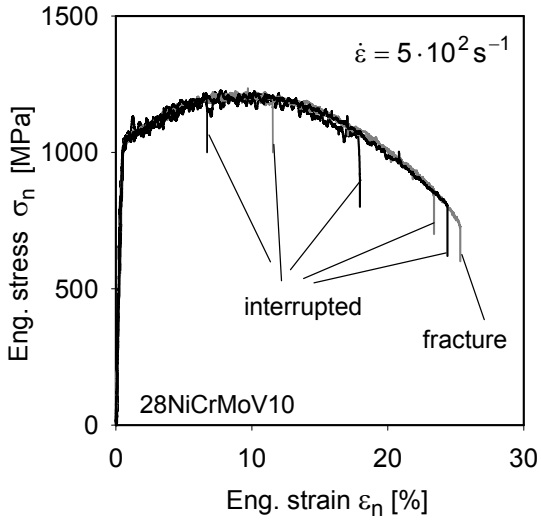

Figure 2: *Stress strain diagrams of interrupted tests of low alloyed tool steel*

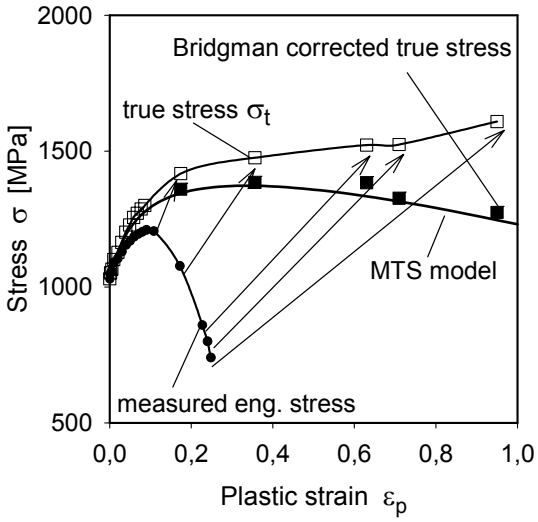

Figure 3: *Comparison of experimental data and MTS model*

Figure 2 shows the results of interrupted tensile tests of specimens with 10 mm gage length at a strain rate of $5 \cdot 10^2$ s^{-1} with a low scatter between six tests interrupted at certain stages of necking. The true stress was determined from the measured force and the true diameter in the necking zone and corrected for the uniaxial state according to Bridgman [6]. Comparing these results with the calculated curve of the MTS model extrapolated from UTS to the fracture strain, a good agreement was achieved, Figure 3. This offers the important advantage to establish high rate true stress-true strain relations up to the necking strain. This is mostly 10fold to the homogenous strain without friction effects, which disturb results of upsetting tests.

Figure 4 compares the experimental data at different strain rates with the calculated flow curves from the MTS model. Because of the effect of dynamic strain aging the experimental data at the strain rate of 10^{-3} s^{-1} exceeds the flow curve calculated with MTS model eq. (1). Considering the effect of dynamic strain aging by using the modified form of the MTS model eq. (4), a good agreement between the experimental data and the calculated curve (dashed curve) results.

The calculated flow stresses with the modified MTS model eq. (4) are plotted in figure 5 as a function of the temperature at different strain rates. The effect of dynamic strain aging shifts to a higher temperature due to higher strain rates.

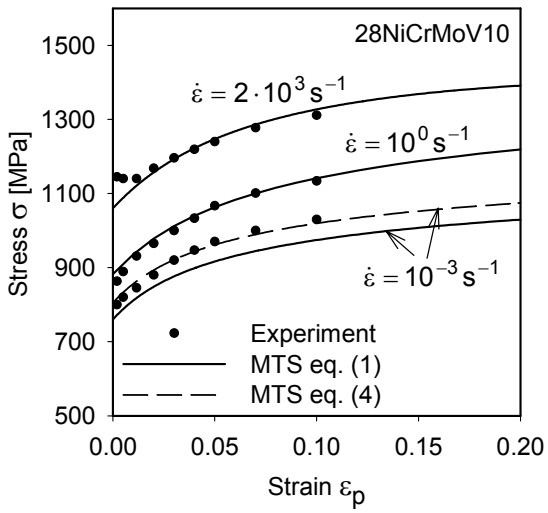

Figure 4: *Stress-strain behavior from low to high rates of strain and improvement of the MTS model by dynamic strain aging*

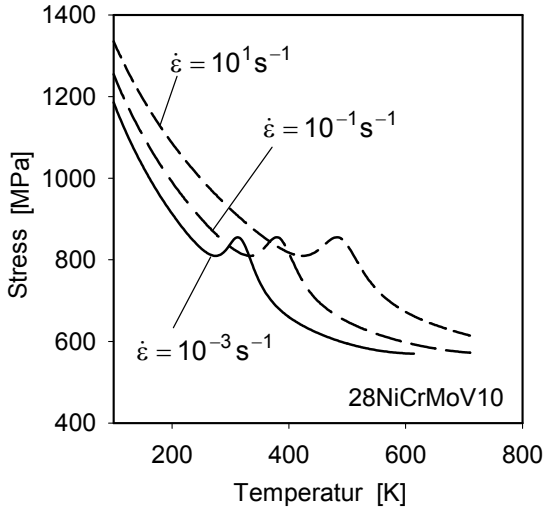

Figure 5: *Influence of dynamic strain aging at different temperature and strain rates*

4.2 Ductile failure

Notched tensile specimens were used with different stress states in the root section to characterize the ductile failure of the investigated low alloy steel. The stress triaxiality must be determined at the fracture initiation. Therefore, FEM computations were performed to calculate the development of the stress triaxiality σ_m/σ_v. The computations were carried out with LS-DYNA 3D explicit with a striking velocity of 5 m/s and 25 m/s and also as an implicit calculation to simulate the quasistatic loading. A quarter model is used for each notch radius and also for the unnotched specimen. The MTS model was used for the input of the material data.

To show the effect of strain hardening on the development of stress triaxiality, an implicit computation was carried out with a notch radius of 2.5 mm with two different flow curves. The first is an elastic-ideal plastic curve $d\sigma/d\varepsilon = 0$ and the second is an elastic one with a strong linear strain hardening $d\sigma/d\varepsilon = 500$ MPa. The yield stress (elastic limit) for both curves is 500 MPa. The results of these computations show that the high strain hardening yields to smaller stress triaxiality, figure 6.

The computed stress triaxiality of notched und unnotched specimens is represented in dependence of the equivalent strain, figure 7. The arrows represent the experimentally determined effective strain at the fracture initiation under quasistatic loading. It can be noticed that the stress triaxiality affects the failure behavior much more than the strain rate.

The influence of strain rate on the effective fracture strain is shown in figure 8 for the unnotched and notched cases. With increasing strain rate the local fracture strain of unnotched specimens decreases slightly up to $\dot{\varepsilon} \approx 10^1$ s^{-1}, then it increases clearly beyond $\dot{\varepsilon} > 10^3$ s^{-1}. In some metallic materials the so-called strain rate embrittlement was observed [1,8]. At high strain rates the ductility of metals can also increase due to the adiabatic heating resulting from the transformation of the deformation energy into heat.

When the influence of the adiabatic heating is stronger than of the strain rate, then the fracture strain increases at high strain rates. The local fracture strain of the notched specimens decreases only slightly with increasing strain rate. The main influence is due to the stress triaxiality, not due to the strain rate.

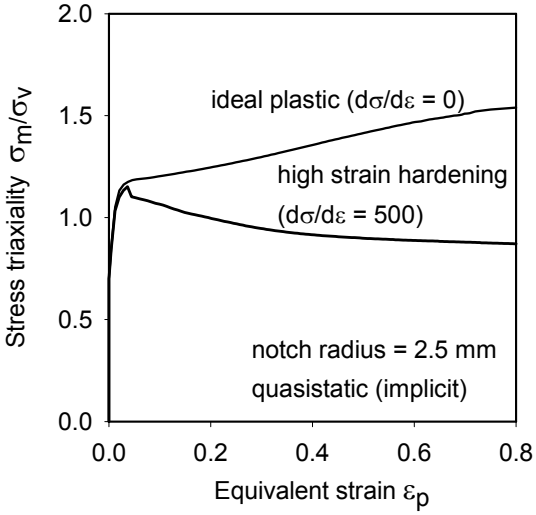

Figure 6: *Influence of strain hardening on the stress triaxiality (FEM solution)*

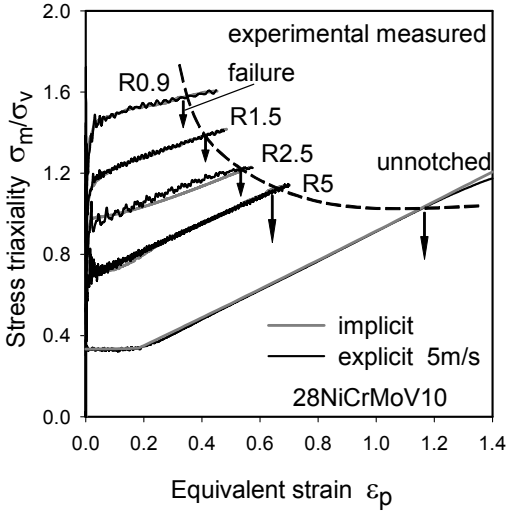

Figure 7: *Stress triaxiality of different notch radii under quasistatic and dynamic loading (FEM)*

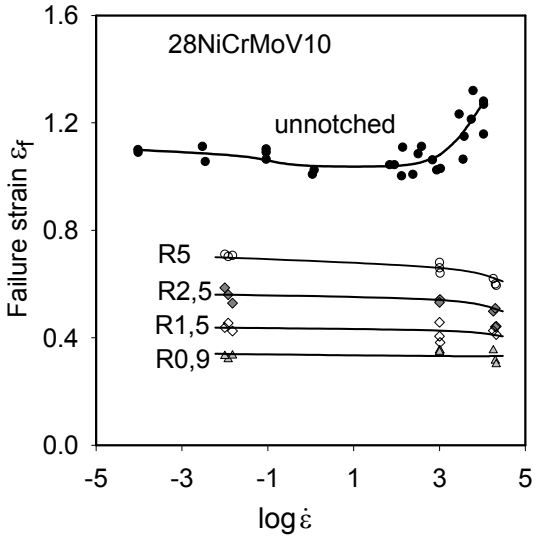

Figure 8: *Dependence of the fracture strain on the strain rate*

5 Conclusions

The material behavior of a low alloy steel in a wide range of strain rates was described with the MTS model. Adding an extra stress part to the MTS model, the effect of the dynamic strain aging was considered, too.

With stopped tests it was proven that the complete tensile test is usable for evaluating flow stresses with the MTS model, even up to fracture, but without friction influences. This is an important step forward for the simulation community because upsetting tests are never free from unknown friction effects.

The ductile failure depends considerably on the stress triaxiality. The strain rate plays a minor role.

References

[1] *Meyer, L. W.:* Constitutive equations at high strain rate. In: Shock wave and high strain rate phenomena in materials, Eds.: Meyers, M. A.; Murr, L. E. and Staudhammer, K. P., Marcel Dekker, New Yourk, 1992, p.657-673.

[2] *Follansbee, P. S.; Kocks, U. F.:* A constitutive description of the deformation of copper based on the use of the mechanical threshold stress as an internal state variable. Acta Metall., 36, 1988, p.81-93.

[3] *Follansbee, P. S.; Gray, G. T.:* An analysis of the low temperature, low and high strain-rate deformation of Ti-6Al-4V. Metall. Trans., 20A, 1989, p.863-874.

[4] *Follansbee, P. S.; Huang, J. C.; Gray, G. T.:* Low-temperature and high-strain-rate deformation of Nickel and Nickel-Carbon alloys and analysis of the constitutive behaviour according to an internal state variable model. Acta Metall., 38, 1990, p. 1241-1254.

[5] *Meyer, L. W.:* Werkstoffverhalten hochfester Stähle unter einsinniger dynamischer Belastung. Dissertation, Universität Dortmund, 1982.

[6] *Bridgman, P. W.*: The stress distribution at the neck of a tension specimen. Transactions of the A.S.M., 32, 1944, p.553-572.

[7] *Burgahn, F.:* Einsinniges Verformungsverhalten und Mikrostruktur ausgewählter Stähle in Abhängigkeit von Temperatur und Verformungsgeschwindigkeit. Dissertation, Universität Karlsruhe (TH), 1991.

[8] *Orava R. N.:* The effect of dynamic strain rates on room temperature ductility. 1. Int. Conf. High Energy Forming, Estes Park, Denver, Col., USA,, 1967.